STUDY OF HIGH-FREQUENCY IMPEDANCE OF SMALL-ANGLE TAPERS AND COLLIMATORS*

G. Stupakov, SLAC National Accelerator Laboratory, Menlo Park, CA, USA

B. Podobedov, Brookhaven National Laboratory, Upton, NY, USA

Abstract

Collimators and transitions in accelerator vacuum chambers often include small-angle tapering to lower the wake-fields generated by the beam. While the low-frequency impedance is well described by Yokoya's formula (for axisymmetric geometry), much less is known about the behavior of the impedance in the high frequency limit. In this paper we develop an analytical approach to the high-frequency regime for round collimators and tapers. Our analytical results are compared with computer simulations using the code ECHO.

INTRODUCTION

The impedance of small-angle axisymmetric tapers with perfectly conducting walls was first computed analytically by Yokoya in the limit of low frequencies [1]. In this limit the longitudinal impedance is purely imaginary, which means that the beam does not lose energy to radiation. Later works [2, 3] generalized Yokoya's approach for rectangular and elliptical cross sections of the transitions. In the opposite limit of very high frequencies a so-called optical model has been developed [4, 5] which predicts a real longitudinal impedance. Simulations show, however, that there is a large range of frequencies between Yokoya's theory and the optical impedance where both theories fail to provide an accurate result. In this paper we address this intermediate regime between the two limiting theories. This paper uses the method developed in an earlier paper by one of the authors [6], which attempted to solve this problem, but failed to take into account the effect of mode transformation in transition regions.

In this paper we consider the geometry of an axisymmetric collimator shown in Fig. 1. It consists of two identical conical tapers of length l connected by a section of a
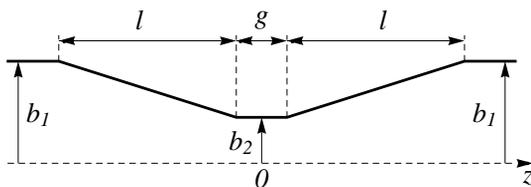

Figure 1: Geometry of an axisymmetric collimator.

cylindrical waveguide of length g. The radius of the pipes outside of the collimator is b_1, and the radius of the pipe between the tapers is b_2. We use cylindrical coordinate system r, z, ϕ with the origin of the coordinate z situated in the middle of the collimator. The system is then symmetric with respect to reflection in the plane $z = 0$. The radius of the collimator $b(z)$ as a function of z is defined by

$$b(z) = \begin{cases} b_2, & 0 < |z| < \frac{g}{2}, \\ b_2 + (b_1 - b_2)\frac{|z|-g/2}{l}, & \frac{g}{2} < |z| < l + \frac{g}{2} \\ b_1, & |z| > l + \frac{g}{2}. \end{cases}$$ (1)

Throughout this paper we assume that the angle of the collimator α is small, $\alpha = \arctan(b_1 - b_2)/l \approx (b_1 - b_2)/l \ll 1$.

We assume that a beam propagates along the axis of the collimator at the speed of light. Our goal is to calculate the longitudinal impedance of the collimator.

THE METHOD

We use a method of eigenmodes, in which the electromagnetic radiation field of the beam is represented by a sum of modes of the empty waveguide. It is based on calculation of the energy radiated by the image currents induced by the beam in the walls of the waveguide. In the absence of other losses, the radiated energy is equal to the energy loss of the beam and can be related to the real part of the impedance. The imaginary part of the impedance can then be found using the Kramers-Kronig relations between the imaginary and real parts of the impedance.

The detailed description of the method is presented elsewhere [7]; here we limit ourselves to a brief outline of our approach.

The Fourier component of the beam current is (we assume the $e^{-i\omega t}$ time dependence in what follows)

$$I_\omega = I_0 e^{ikz},$$ (2)

where ω stands for frequency, I_0 is the amplitude of the current harmonic and $k = \omega/c$. Let us denote the time-averaged intensity of radiation of this current from the collimator region by P_ω. The real part of the impedance is then given by the following relation (see, e.g., [8])

$$\mathrm{Re}Z(\omega) = \frac{2P_\omega}{I_0^2}.$$ (3)

The radiation is due to the image currents induced in the perfectly conducting walls in the taper regions where the

05 Beam Dynamics and Electromagnetic Fields

walls are not parallel to the z-axis. It is convenient to represent the total electric field of the beam inside the taper as a sum of the vacuum field, $\boldsymbol{E}^{\mathrm{vac}}$, and the radiation field $\boldsymbol{E}^{\mathrm{rad}}$, $\boldsymbol{E} = \boldsymbol{E}^{\mathrm{vac}} + \boldsymbol{E}^{\mathrm{rad}}$, where for an on-axis beam

$$\boldsymbol{E}^{\mathrm{vac}} = \hat{\boldsymbol{r}} \frac{2I_0}{rc} e^{ikz}, \tag{4}$$

with $\hat{\boldsymbol{r}}$ being a unit vector in the radial direction of the cylindrical coordinate system.

The radiation field $\boldsymbol{E}^{\mathrm{rad}}$ satisfies Maxwell's equation with the boundary condition that requires the tangential component of the total electric field on the wall to vanish $\boldsymbol{E}_t^{\mathrm{rad}}|_{\mathrm{wall}} = -\boldsymbol{E}_t^{\mathrm{vac}}|_{\mathrm{wall}}$. Inside the waveguide, the radiation field excited by the wall currents can be represented as a sum of eigenmodes,

$$\boldsymbol{E}^{\mathrm{rad}} = \sum_n a_n \boldsymbol{E}_n^+, \tag{5}$$

where a_n is the amplitude and $\boldsymbol{E}_n^+$ is the electric field of the n-th eigenmode, propagating in the positive direction of the z axis. A similar expansion in terms of the amplitudes a_n is also valid for the magnetic field. Note that in general case, the sum in (5) also includes modes $\boldsymbol{E}_n^-$ propagating in the backward direction [9]. However, in the limit of high frequency, the modes that make a dominant contribution to the impedance propagate in the forward direction, and the backward propagating modes can be neglected.

Having found the modal expansion coefficients a_n at the exit from the collimator $z = g/2 + l$, (see [7] for details), we can determine the spectral power of radiation $P_\omega = \sum_n P_n |a_n|^2$, where P_n is the energy flow in the n-th mode of unit amplitude. This in turn allows us to find the impedance, as given by Eq. (3).

To calculate the excitation of electromagnetic field by the beam, one needs to know the eigenmodes of the complete waveguide. Analytical expressions for eigenmodes are available for cylindrical and conical waveguides, however, there is no a compact expression for eigenmodes of a collimator shown in Fig. 1. Moreover, a single conical mode that propagates in the left taper of the collimator, experiences transformation at the transition to the straight central section, generating several modes in the cylindrical waveguide. Each of these modes, in turn, experiences a transformation at the second transition from the cylindrical waveguide to the right taper, resulting in multiple conical modes in the right taper.

For calculation of the longitudinal impedance one only needs axisymmetric TM modes. In the cylindrical central part of the collimator, the modes propagating in the positive direction, $\boldsymbol{E}_n^+, \boldsymbol{H}_n^+$, are given by the familiar equations

$$E_{z,n}^+ = \frac{j_n^2}{b_2^2} J_0\left(j_n \frac{r}{b_2}\right) e^{i\phi_n(z)}$$

$$E_{r,n}^+ = -\frac{ij_n k_n}{b_2} J_1\left(j_n \frac{r}{b_2}\right) e^{i\phi_n(z)}$$

$$H_{\phi,n}^+ = -\frac{i\omega j_n}{b_2 c} J_1\left(j_n \frac{r}{b_2}\right) e^{i\phi_n(z)} \tag{6}$$

where n is the mode index, $n = 1, 2, \ldots$, J_0 and J_1 are the Bessel functions, j_n is the n-th root of J_0, and $k_n = (\omega^2/c^2 - j_n^2/b_2^2)^{1/2}$. The phase of the mode is equal to $\phi_n(z) = k_n z$.

Analytical expressions for eigenmodes of the electromagnetic field are also available for conical geometry (see, e.g., [9]). In the general case of arbitrary cone angle α and arbitrary frequency ω, they involve the Legendre and Bessel functions. In the limit of high frequency, it turns out that only the modes that propagate at small angles to the axes of the system make a dominant contribution to the impedance (so called paraxial approximation, see [11]). We use a simplified version of these functions valid in the limit of small angle α and high frequency ω. In this limit, the conical eigenmodes (which we mark by the tilde below) are similar to the cylindrical ones, and, in our cylindrical coordinate system, they can be written as follows

$$\tilde{E}_{z,n}^+ = \frac{j_n^2}{b^2} J_0\left(j_n \frac{r}{b}\right) e^{i\phi_n(z) + ikr^2/2R(z)}$$

$$\tilde{E}_{r,n}^+ = -\frac{ij_n k}{b} J_1\left(j_n \frac{r}{b}\right) e^{i\phi_n(z) + ikr^2/2R(z)}$$

$$\tilde{H}_{\phi,n}^+ = -\frac{i\omega j_n}{bc} J_1\left(j_n \frac{r}{b}\right) e^{i\phi_n(z) + ikr^2/2R(z)}, \tag{7}$$

where the phase ϕ_n is now determined from the differential equation $d\phi_n/dz = [\omega^2/c^2 - j_n^2/b(z)^2]^{1/2}$. The factor $R(z)$ in the above equations is the curvature radius of the spherical wavefronts of the modes in the conical regions; it is equal $R(z) = [\arctan b'(z)/b(z)]^{-1} \approx b(z)/b'(z)$. Note that due to the linear dependence of $b(z)$ in the tapers, $b' = \mathrm{const}$. The sign of R is important: it is negative in the left taper, corresponding to converging wavefronts of the modes, and is positive in the right taper, where the wavefronts are diverging from the center of the collimator. For the phase $\phi_n(z)$ in (7) we have $\phi_n(z) = \int_0^z [\omega^2/c^2 - j_n^2/b(z')^2]^{1/2} dz'$.

The small angle of the collimator, as was pointed out in [6], allows one to neglect the reflection of eigenmodes at the transitions between the cylindrical and conical regions. However, it does not preclude mode transformation at these transitions, and we will account for this below.

NUMERICAL RESULTS

The impedance calculation algorithm described above was implemented in Mathematica [12]. For illustration purposes we have chosen the following collimator geometry: $l = g = 3$ cm, $b_1 = 2b_2 = 0.5$ cm, so that the collimator angle is $\alpha = 4.7$ degrees. Real part of the impedance computed from the beam pipe cutoff, $f_c = j_1 c/2\pi b_2 = 46$ GHz, up to the frequency $f_{\max} = 3.9$ THz is shown in Fig. 2 in solid blue. At higher frequencies this impedance approaches the optical model value, $Z_{\mathrm{opt}} = (Z_0/\pi) \log(b_1/b_2) = 83\Omega$.

While our algorithm directly finds only the real part of impedance, we can find the imaginary part by making use of causality, that relates imaginary and real parts of the
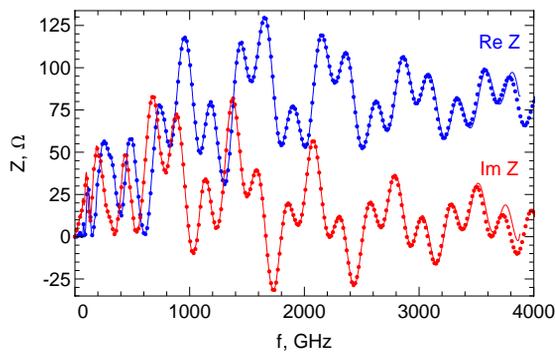
Figure 2: Collimator impedance: present theory is shown with solid line, the results of simulations with ECHO are shown with dots.

impedance via the Hilbert transforms (Kramers-Kronig relations) [8]. To proceed, we need to define Re Z for all frequencies, so we set it to zero below f_c, and set it equal to the optical model value above f_{max}. Im Z calculated by the Hilbert transform of this Re Z is shown in Fig. 2 in solid red. Below the cutoff frequency it ends up very close to the Yokoya value. For comparison, we plot impedances calculated from a Fourier-transformed wakepotential of a $\sigma_z = 20\,\mu m$ Gaussian bunch computed by the code ECHO [13]. One can see a very good agreement between our approach and the ECHO results.

Since our algorithm allows one to accurately find the impedance over a very broad frequency range, we can use inverse Fourier transform to reconstruct the wakepotential of a short bunch. For instance, for a Gaussian bunch with rms length $\sigma_z = 100\,\mu m$ we obtain the wakepotential shown in Fig. 3, plotted with the ECHO result for comparison. Again, we observe a perfect agreement between the two.
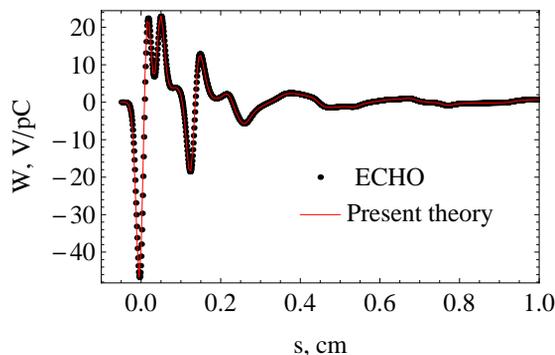

Figure 3: Wakepotential of a $\sigma_z = 100\,\mu m$ bunch.

Finally, in Fig. 4 we present the loss factor and the maximum absolute value of the wakepotential as a function of bunch length. As we expect from the optical model, for short bunches, both quantities scale as σ_z^{-1}, while in

the opposite, Yokoya regime, $|W(s)|_{max} \propto \sigma_z^{-2}$ and the loss becomes exponentially small. In the intermediate region (roughly 2 magnitude orders in σ_z with corresponding changes of 3 or more orders in magnitude in $|W(s)|_{max}$ and k_{loss}) the scaling is more complex, and, to our knowledge, it is not described by any existing analytical treatments. Our new approach comfortably fills this gap.
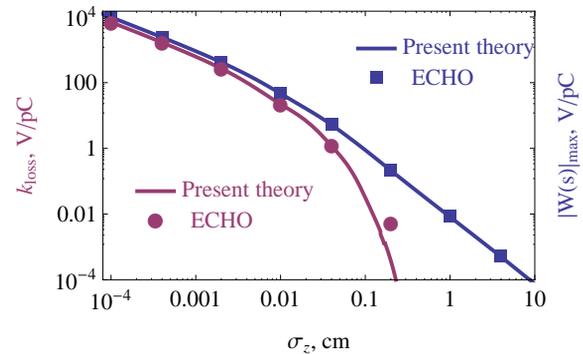

Figure 4: Loss factor and maximum of the wakepotential.

In conclusion, we developed a novel analytical approach to find the impedance of (small angle) tapered collimators in axially symmetric geometry. Impedance can be found over a very broad frequency range, from DC to high-frequency optical model limit, thus allowing one to reconstruct the wakepotential of short bunches. We note that this algorithm is also applicable to convex (cavity-like) structures, and, with some modifications, small angle requirement can be dropped. Extension to 3D geometries will be investigated in the future.

REFERENCES

[1] K. Yokoya, Tech. Rep. SL/90-88 (AP) (CERN, 1990)

[2] B. Podobedov and S. Krinsky, PRST-AB **10**, 074402 (2007)

[3] G. Stupakov, PRST-AB **10**, 094401 (2007)

[4] G. Stupakov, *et al.* PRST-AB **10**, 054401 (2007)

[5] K. Bane, *et al.* PRST-AB **10**, 074401 (2007)

[6] G. Stupakov, Preprint SLAC-PUB-7039 (SLAC, 1995)

[7] G. Stupakov and B. Podobedov, Preprint SLAC-PUB-14093 (SLAC, 2010)

[8] A. W. Chao, *Physics of Collective Beam Instabilities in High Energy Accelerators* (Wiley, New York, 1993)

[9] L. A. Vainshtein, *Electromagnetic Waves* (Radio i svyaz', Moscow, 1988) in Russian

[10] R. E. Collin, *Field Theory of Guided Waves*, 2nd ed. (IEEE Press, New York, 1991)

[11] G. Stupakov, New Journal of Physics **8**, 280 (2006)

[12] Wolfram Research, Inc., *Mathematica*, version 7.0 ed. (Wolfram Research, Inc., 2008)

[13] I. Zagorodnov and T. Weiland, PRST-AB **8**, 042001 (2005)